

1986

Studies on Pressure Drops in Air Flowing Through Inside Tubes with Frosting

K. Katsuta

I. Tshihara

Follow this and additional works at: <http://docs.lib.purdue.edu/iracc>

Katsuta, K. and Tshihara, I., "Studies on Pressure Drops in Air Flowing Through Inside Tubes with Frosting" (1986). *International Refrigeration and Air Conditioning Conference*. Paper 19.
<http://docs.lib.purdue.edu/iracc/19>

This document has been made available through Purdue e-Pubs, a service of the Purdue University Libraries. Please contact epubs@purdue.edu for additional information.

Complete proceedings may be acquired in print and on CD-ROM directly from the Ray W. Herrick Laboratories at <https://engineering.purdue.edu/Herrick/Events/orderlit.html>

STUDIES ON PRESSURE DROPS IN AIR FLOWING THROUGH INSIDE TUBES WITH FROSTING

ISAO ISHIHARA and KATSUTARO KATSUTA
Kansai University, Department of Mechanical
Engineering, Suita Osaka 565 (Japan)

1. INTRODUCTION

When the humid air flows through the inside tubes, the walls of which are cooled at low temperature, the frost layers are formed and they offer resistances to the flow. Their resistances are mainly caused by contractions of the air stream; that is, blockage of the flow due to the frost accumulations, and the flow frictions on the rough surfaces of the frost layers.

To investigate experimentally the pressure drops due to these resistances, the configurations of the frost layers formed at constant flow rates are observed, and then the pressure drops and the thickness and mass of the frost layers are measured.

The loss coefficients of the blockage were obtained and the roughness of the frost layer surface were evaluated hydrodynamically.

2. EXPERIMENTAL APPARATUS AND PROCEDURES

Fig.1 shows the test tube. The tube is mounted horizontally and divided into the two parts: upstream tube and downstream one. They have 21mm I.D. and 500mm and 1000 mm in length respectively. They are cooled at about -20°C by the cold brine flowing through the annular passage and then the frost deposit on the inside wall of tube.

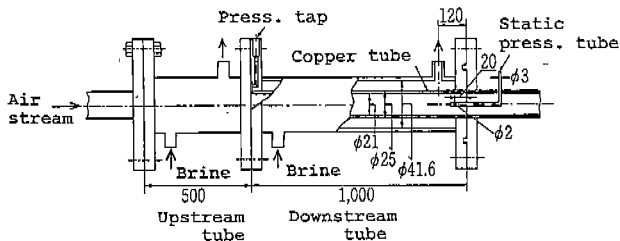


Fig.1 Test tube

Uncooled tubes with 2m length and 21mm I.D. are connected with the both sides of the two parts of test tube by bakelite flanges. Therefore the air flow entering into the tube is considered to have a fully developed velocity profile.

Pressures are measured by strain gauge type pressure gauges at $x=500$ and 1980mm , where x is distance from the inlet of the test tube. The pressures at the inlet and outlet are obtained by measuring pressure distributions in the uncooled tubes.

The air flow from a centrifugal fan is maintained a constant flow rate during frosting in each run. Their average velocities are $U_0=5, 10$ and 15 m/s under no-frosted condition and the corresponding Reynolds numbers are nearly equal to $Re_d=6.3 \times 10^3, 1.4 \times 10^4$ and 2.1×10^4 .

There are five intervals in each run: 15, 30, 45, 60, 90 and 120 minutes under the same condition. If the constant flow rate can not be maintained any longer, measuring is stopped.

At the end of each interval, the test tube (both the upstream and downstream tube) is removed from the apparatus and then the frost layer thicknesses are measured at the inlet, middle ($x=500\text{mm}$) and outlet of the tube by a cathetometer. The mass of the frost deposition after melting is measured by a precision balance.

3. EXPERIMENTAL CONDITIONS

The air conditions for each run are shown in the humid air diagram Fig.2 together with frosting time t , initial flow velocity U_0 and brine temperature θ_b . As shown in it, runs 3 to 6 were carried out under lower vapor concentrations in the air stream. In runs 7 to 9, the test tube of 1 m in length was used.

4. RESULTS AND DISCUSSION

4.1 Configuration of frost layer

Fig.3 shows a photograph of vertical cross section of the frost layer at the entrance region, and black lines direct its inner profile. The frost layer has a uniform thickness throughout the tube surface at the first period of frost formation or in the case of lower vapor concentration of air, that is a uniform frost deposition. In this figure, however, the blockages appear. Such a configuration will be called the blockage type deposition hereafter.

The first blockage takes place at about $x=20\text{mm}$ downstream from the entrance and the frost layer in this position is thicker at the bottom of the tube than at the top because of gravitational force. Reattachment of the shear flow departed from the blockage part makes the second blockage at $x=80-130\text{mm}$. However, the uniform frost layer is found to exist at down-stream from this region.

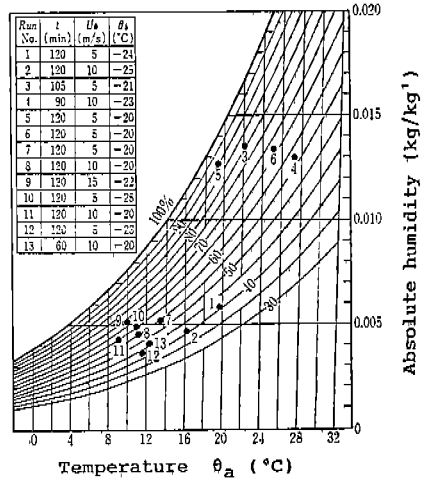


Fig.2 Experimental conditions

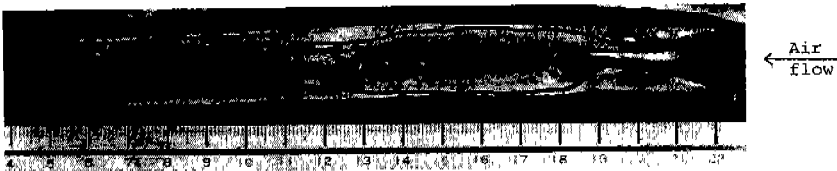


Fig.3 Vertical cross section of frost layer (Run 6, $t=120\text{mm}$)

4.2 Flow channel model and pressure drops

(1) Flow channel model

As described previously, the frost deposition transit from the uniform deposition to the blockage type deposition, and accordingly air flow patterns change.

Although distribution of the frost layer thickness is complex in the blockage type deposition, it is assumed that the shape of flow channel can be replaced with a simplified one as shown in Fig.4, and then to be considered the pressure drops in the each parts of the tube respectively. In this figure, a denotes the inlet, d the middle, g the outlet and b the blockage region.

As mass of the deposited frost is less than 1 percent of mass flow rate of the air stream under our experimental conditions, negligible is the pressure drop caused by momentum change of the flow due to it.

Total pressure drop ΔP_t in the test tube is given by the following equation :

$$\Delta P_t = \Delta P_{ac} + \Delta P_f + \Delta P_{eg} \quad (1)$$

where, ΔP_{ac} is the pressure drop due to the blockage between a and c, and equal to the sum of ΔP_{ab} and ΔP_{bc} . ΔP_{eg} is the recovery of the pressure due to enlargement of the flow channel at the tube end. ΔP_f is frictional pressure loss in the test tube.

(2) Loss coefficient of enlargement at outlet of tube

At the outlet, cross-sectional area of the air flow changes from the test section with frosting to no frosted tube section. Therefore, the flow velocity is reduced and then the pressure is recovered.

This pressure recovery is given by

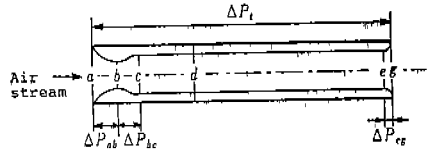


Fig.4 Flow channel model

$$\Delta P_{eg} = \{ (1 + \zeta_e) U_g^2 - U_e^2 \} \rho / 2 \quad (2)$$

where ζ_e is the loss coefficient due to enlargement, ρ is density of the air, and U_g and U_e denote average flow velocities at e and g respectively.

Relationship between the coefficient ζ_e measured by the pressure drop and the frost layer thickness l_f at e was closely correlated by Carnot's equation /1/ :

$$\zeta_{et} = (F_g / F_e - 1)^2 \quad (3)$$

where F is cross sectional area.

(3) Pressure drop at blockage region

The pressure drop due to blockage consists of the combination of enlargement and contraction. This is defined by

$$\Delta P_{ac} = \{ (1 + \zeta_c) U_c^2 - U_g^2 \} \rho / 2 \quad (4)$$

By applying the value given by Fujimoto /1/ and Carnot's equation to the loss coefficient for contraction and enlargement of flow respectively,

$$\zeta_{ct} = 0.052 + (F_c / F_b - 1)^2 \quad (5)$$

is obtained. In the case of the uniform deposition, the second term in the equation is neglected.

Table 1 indicates a fairly good agreement between the experimental values ζ_c and predicted ones ζ_{ct} .

(4) Frictional pressure loss

The pressure loss ΔP_f is obtained by

$$\Delta P_f = \Delta P_t - \Delta P_{ac} - \Delta P_{eg} \quad (6)$$

and given by using friction factor λ_f as follows:

$$\Delta P_f = 8 \lambda_f G^2 l / (\pi^2 \bar{d}_f^5 \bar{\rho}) + 8 G^2 \{ 1 / (\rho_0 d_{f0}^4) - 1 / (\rho_i d_{fi}^4) \} / \pi^2 \quad (7)$$

where the second term in this equation is the pressure drop caused by momentum change of the air flow. G denotes mass flow rate of the air stream, d_f is average diameter of the frosting tube and l is length of the tube. Subscript i, o and - denote inlet, outlet and average in the longitudinal direction respectively.

Table 1. Loss coefficient of contraction

Run	U_0 m/s	t min	l_{fb} mm	l_{fe} mm	ΔP_{ac} Pa	ζ_c $\times 10^{-2}$	ζ_{ct} $\times 10^{-2}$
11	5.0	15	1.0	0.8	7.0	6.1	5.4
		30	1.5	1.0	9.6	9.0	6.5
		60	2.2	1.7	17.5	7.7	6.7
		120	2.8	2.1	14.6	7.8	8.8
12	10.0	15	1.1	1.0	48.5	19.0	5.3
		30	1.5	1.3	48.0	5.6	5.4
		45	1.8	1.7	72.0	6.4	5.3
		60	1.9	1.8	75.0	5.8	5.3

4.3 Pressure drops

Fig.5 shows relationship between the pressure drops and frosting intervals.

ΔP_t indicates a total pressure drop in 1.5m test tube, and ΔP_{ac} and ΔP_{eg} are calculated by substituting measured frost layer thickness into eqs.(4), (5) and (2), (3) respectively.

In this figure, ΔP_t at t=0 is equal to that for a smooth tube without frosting. As the frost layer surfaces become rougher at the beginning of frost growth, ΔP_t increases considerably. And ΔP_t increases monotonously with reducing sectional area of the flow. As the transition from the uniform deposition to the blockage type one occurred at about 60 minutes in this run, the pressure drop increases rapidly after that time. This run was obliged to be stopped at 105 minutes because a constant flow rate was not kept any longer.

Friction loss ΔP_f shown by a alternate long and two short dashes line in Fig.5 accounts for greater part of ΔP_t during the uniform deposition. However, after transition to the blockage type, ΔP_f decreases and becomes less than ΔP_{FB} which is calculated by Blasius expression for smooth surface. This is seemed to be due to overestimate ΔP_{ac} , so that the simplified flow channel model changes to an inadequate one after a period for the blockage type deposition in the upstream tube.

(1) Frictional pressure loss

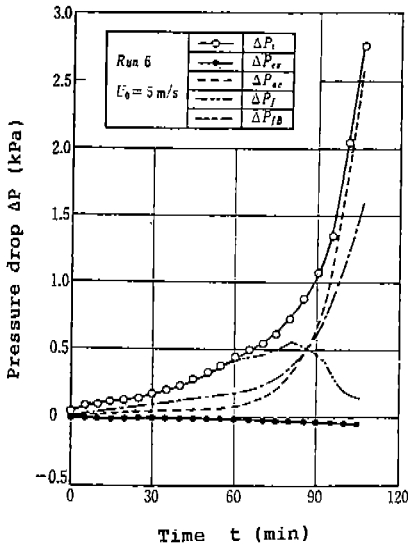


Fig. 5 Pressure drop vs time

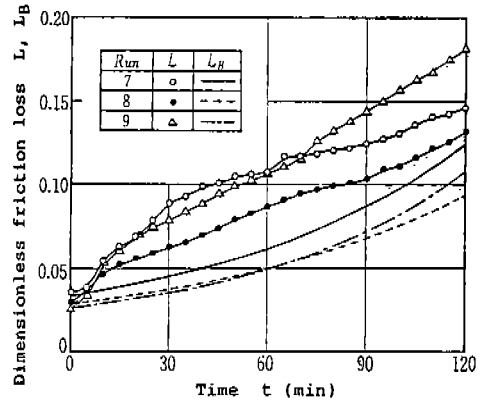


Fig. 6 Dimensionless frictional pressure loss for 1m-tube

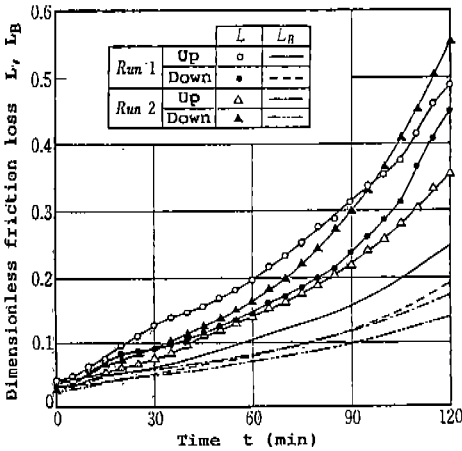


Fig. 7 Dimensionless frictional pressure loss for low concentration

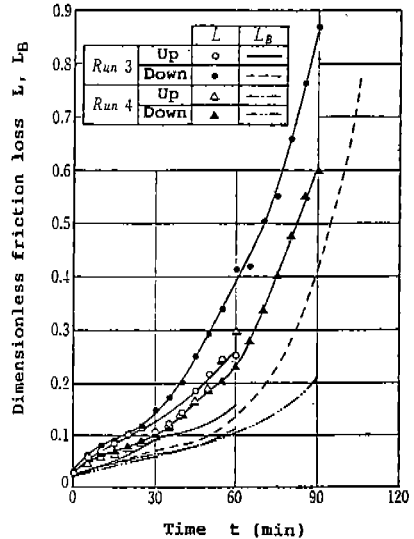


Fig. 8 Dimensionless frictional pressure loss for concentration

For more detail investigation, the friction losses in the upstream and downstream tube ; ΔP_{F1} and ΔP_{F2} were measured. And the relationships between dimensionless loss $L = \Delta P_F / \{\rho_a U_0^2 l / (2d_0)\}$ and time are given in Figs. 6, 7 and 8. Furthermore L_B is defined by $\Delta P_{FB} / \{\rho_a U_0^2 l / (2d_0)\}$, where d_0 denotes the inner diameter of the tube ($=21\text{mm}$) and ρ_a is air density at the normal condition ($=1.251\text{kg/m}^3$).

The uniform depositions are shown to be kept throughout runs in Figs. 6 and 7, while the transition to the blockage type deposition occurred at runs 3 and 4 in Fig. 8. Under the condition which are constant mass flow rate is maintained during each run, L is subject to flow velocity change caused by the growth of the frost layer and stands for characteristics of the frost surface. As reduction rate of the flow area due to the frost growth is small at the early period of the growth, it is considered that increments of L are caused mainly by the rough frost surface. In Figs. 6 and 7, they are shown within 30 minutes and in Fig. 8, at the earlier period because of more rapid growth of the frost.

In these figures, L is equal to L_B at $t=0$ and afterwards L becomes greater than

L_B with increasing the thickness of frost layer. However, the frost surface is tend to be smooth after the frost grew to some extent.

Dense frost layer makes the layer surface into a smooth one and L has a tendency to approach to L_B . However, in the case of low vapor concentration in the air stream, the frost layer in the downstream region keeps to be in a porous and coarse structure. Hence the differences between L and L_B increase with growth of the frost.

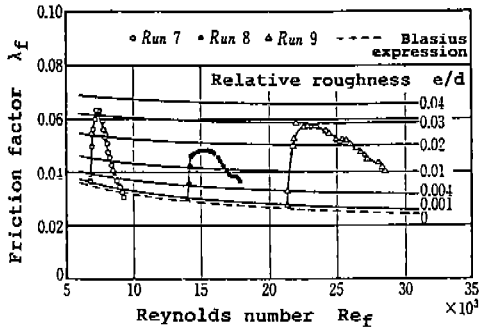


Fig.9 Friction factor of frost surface for 1m-tube

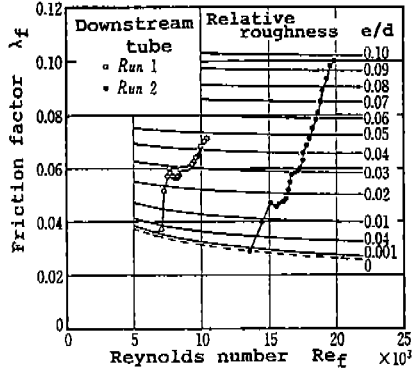


Fig.10 Friction factor of frost surface for low concentration

(2) Friction factor

The friction factors for the frost surface λ_f , which are derived from eq.(7), are shown with Reynolds number Re_f in Figs.9,10 and 11. As Re_f is defined by using flow velocity U_f and diameter d_f in the frosted tube, the values of Re_f increase as the frost layer grows.

In Fig.9 the results of runs carried out by using the test tube with whole length 1.0m, and also in Figs.10 and 11 those for the downstream tube of 1.0m length are shown.

After the friction factors increase and reach the maximum values with growth of the frost, the frost surfaces become smooth again and the factors are tend to approach to the values of Blasius expression. This tendency is seemed to be corresponded to the general process of the frost growth.

In the case of lower concentration of water vapor, as shown in Fig.10, the frost layer grows on keeping the coarse structure at the downstream region, so that the factor increases continuously and its tendency differs from that in Fig.9. However, according with close observation to the figure, it is clear that the maximum values exist in the earlier period and the factor increase rapidly after a short reduction lag. Thus the change process of factor values from increasing to reducing via a maximum value corresponds with them shown in Fig.9.

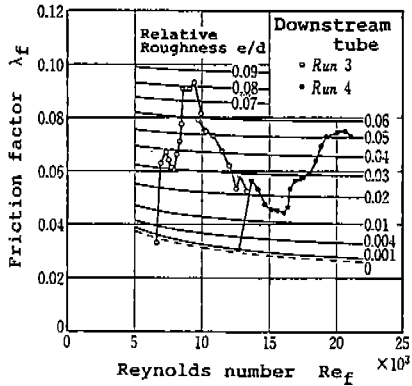


Fig.11 Friction factor of frost surface for high concentration

In the case of higher vapor concentration as shown in Fig.11, the second maximum values appear after following the same tendency as that shown in Fig.10 and then the values of factor decrease. It may be considered that new frost deposits on the smoothed frost layer during the period of increase to the second maximum value. As this new rough surface is smoothed again, the factor decreases. However it is indistinct whether this reaches to the value for the smooth surface or not, because the frost surface in the outlet region of downstream tube is kept to be rough during the run.

The first maximum values of factor were within 30 minutes interval under these experimental conditions. This period of time is equal to that which the frost layer grows rapidly. And the maximum values are nearly equal to 0.06 in spite of discrepancies among experimental conditions.

(3) Roughness of frost layer surface

For trying to evaluate the roughness of the frost surface, Colebrook's equation

is used :

$$1/\sqrt{\lambda_f} = -2\log\{(e_f/d_f)/3.71+2.51/(Re_f\sqrt{\lambda_f})\} \quad (8)$$

Fig.12 illustrates the relationship between relative roughness and frosting time. The roughnesses increase remarkably at the beginning. After a short period when the frost surface becomes smooth with densifying the frost layer, the roughnesses increase again. In such a case as low vapor concentration, the rougher the frost surface becomes, the more frost grows.

As the frost grows rather slowly under low air velocity than high velocity, the maximum roughness appears in a later interval and the value is higher because of lower shear force on the frost surface. However, it is seemed that the air flow makes the surface rough under higher velocity than 10m/s (see Fig.9).

Chen and Rohsenow /2/ have presented a semi-empirical correlation of relative roughness for a "stable" configuration of the frost layer. However, it was not clear whether such a configuration existed in our experiments or not.

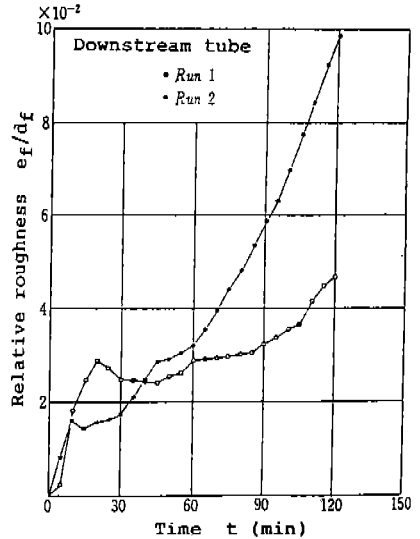


Fig.12 Relative roughness of frost surface

5. CONCLUSIONS

As results of observing the configurations of the frost layer and measuring the frost layer thickness and the pressure drops, the following conclusion are obtained.

- (1) The configurations transit from the uniform frost deposition to the blockage type one with growth of the frost.
- (2) In the case of low humidity of the air stream, the frost at the outlet region keeps its structure porous and coarse during the experimental intervals.
- (3) The three patterns are obtained in the relationships between the relative roughness and frosting time.
- (4) The loss coefficient at the blockage region can be estimated fairly by eq.(5).

REFERENCES

1. Fujimoto, Hydrodynamics, p.86, Yokendo, 1961, (in Japanese)
2. M.M.Chen et al., Journal of Heat Transfer, 1964-8, p.334.

RESUME

Quand l'air humide circule dans les tubes internes dont parois sont réfrigérées a basse température, des couches glacées sont formées et constituent des résistances à la circulation de l'air. Ces résistances sont principalement provoquées par contractions du courant d'air c'est à dire que l'air ne circule plus à cause de l'accumulation de la glace et des forces de friction sur les surface rugueuses des couches gelées.

L'étude expérimentale des variations de pression que provoquent les résistances a été effectuée par observation de la configuration des couches de glace qui se forment à vitesse constante du flux d'air; les variations de pressions ainsi que l'épaisseur et la masse des couches glacées sont ensuite mesurées.

Ceci a permis de déterminer les coefficients de perte par blocage; l'évaluation hydrodynamique de la rugosité de la surface de la couche gelée a été effectuée.

SUMMARY

When humid air flows through the inside of a tube and the walls temperature is low enough, frost will accumulate on the walls. The frost or ice layers offer increased resistance to the air flow. The increased resistance comes from two effects: (1) the decrease in cross sectional areas of the tube caused by the frost layer and (2) the frost layer is generally rougher than the bare tube.

This paper discusses an experimental apparatus to measure the increase in flow resistance. The experimental equipment is used to observe the configuration of the frost layer and to measure pressure drop, frost layer thickness, and mass of frost. Experimental data is presented in the paper.

In addition equations are developed to predict the increase in pressure drop due to frost formation.

The conclusions are: (1) the frost layer progresses from a uniform deposit to non-uniform deposit and finally to complete blockage of the tube, (2) in low humidity air streams, the frost at the outlet is porous and coarse during the entire testing period and (3) the loss coefficient at the blockage region can be estimated using the equation developed in the paper.